Chapter 5
Softening Mechanisms

5.1. INTRODUCTION

The deformation structures developed during thermo-mechanical processing (TMP) are intrinsically unstable so that on annealing, after deformation processing, substructure evolution (excluding classical phase transformations) often occurs by thermally activated processes, leading to a reduction of stored energy. These processes usually induce a significant softening of the plastically deformed material as shown in Figure 5.1.

At low temperatures (in commercial alloys, typically between 0.4–0.5 of the melting temperatures, T_m), recovery dominates and often leads to a slow, logarithmic, decrease of the hardness. At high temperatures (more than $0.7T_m$), recrystallization can occur very rapidly, without much prior recovery. At intermediate temperatures, both mechanisms can contribute significantly to softening.[1]

The associated microstructural changes are defined based on the driving force and the mechanism(s) involved. As shown schematically in Table 5.1, there are two possible driving forces – (i) the stored energy of deformation and (ii) the surface energy or the grain boundary energy. During plastic deformation of crystalline materials, part of the plastic work, typically 1–10%, is stored as microstructural energy, mostly as increased dislocation density; the rest is dissipated as heat. The softening processes are usually separated into recovery, recrystallization and eventually grain growth. The latter two necessarily imply the movement of high-angle boundaries, but recovery involves a set of micromechanisms for the motion and annihilation of point defects and dislocations. It is the combination of driving force and mechanism that differentiates these three 'softening' processes:

- recovery (stored energy and movement of dislocations, either individually or collectively as low-angle boundaries),
- recrystallization (stored energy and movement of high-angle boundaries) and
- grain growth (surface energy and movement of high-angle boundaries).

Given its importance for TMP, the subject has been of major interest for over a 100 years. Table 5.2 provides an overview of some important 'recorded' events of its

---

[1] In very pure metals, recrystallization can occur at much lower temperatures. Pure Cu, for example, may recrystallize at room temperature, as is often observed in microelectronic devices.
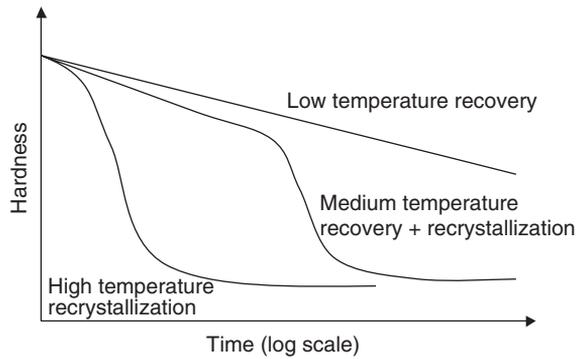
Figure 5.1. Schematic softening kinetics at three temperatures for different combinations of recovery and recrystallization.

Table 5.1. Defining recovery, recrystallization and grain growth, based on the combination of driving force and mechanism.

Mechanism (kinetics)	Driving force (energies)			
	Point defects	Dislocations	Subgrain walls	Grain boundaries
Point defect diffusion	Low temperature			
Dislocation climb		**Recovery**		
Sub-boundary migration and coalascence			High temperature	
Grain boundary migration		**Recrystallization**		**Grain growth**

early history. The field has been well covered by several books and review articles (see, e.g. the literature list). The purpose of this chapter is to provide a 'minimum' knowledge base to students and researchers coming from diverse backgrounds.

5.2. RECOVERY

Softening by recovery can occur if a non-equilibrium concentration of lattice defects is 'reduced', usually by annealing at an appropriate temperature. The defects can be both, point and line defects; but the latter, i.e. dislocations, are more relevant to TMP. Point defects are usually annealed out at relatively low temperatures ($<0.3T_{m}$),

Table 5.2. A few important 'recorded' events of early history, which shaped the present understanding of softening mechanisms. A more extensive list or description can be found in Beck [1963], Hu *et al*. [1990] and Humphreys and Hatherly [1995].

Recorded events of early history	Details
Evidence of structural changes during deformation and subsequent annealing by acoustic anisotropy	Savart [1829]: A simple tuning fork was used for hearing tones, after casting, deformation and annealing of Pb, Sn, Zn and Cu
Change in grain structure during deformation and after annealing by visual inspection	Percy [1864] and Kalischer [1881]: The change in grain structure during annealing was understood as 'crystallization' from the amorphous state
Identification of deformed structure of 'elongated' grains and creation of new grains during annealing – the first recorded use of the term 'recrystallization'	Sorby [1887]: Sorby, using metallographic technique developed by himself, observed 'elongated' grains in a hammered Fe bar and recognized the deformed structure as a 'state of unstable equilibrium', instability resulting in subsequent 'recrystallization'
'Amorphization' of cold-worked material was discounted	Ewing and Rosenhain [1900]: Argued for the 'continuity' of crystalline structure during cold deformation – slip and twinning being the mechanisms of plastic deformation
Separation of the driving force for recrystallization and grain growth	Carpenter and Elam [1920]: Carpenter and Elam established that grain growth is through boundary migration and not through coalescence
Identification of the mechanism for grain boundary movement	Altherthum [1922]: Altherthum distinguished recrystallization and grain growth as 'cold-worked recrystallization' and 'surface tension recrystallization', respectively

i.e. at temperatures below most TMP processes and can usually be ignored except for very low-temperature deformations. Recovery by dislocation annihilation often involves a combination of several micromechanisms (see Table 5.1). The ratio of recovery to recrystallization, however, depends on several factors – strain, annealing temperature and material. The effect of temperature is illustrated schematically in Figure 5.1. Recovery dominates the low-temperature regime, while recrystallization usually occurs rapidly at higher temperatures. Even at higher temperatures, however, there is always some recovery before recrystallization, recovery kinetics being faster than that of low temperatures.

For single phase materials, the stacking fault energy (SFE) also has a strong influence on the amount of recovery; in deformed high-SFE metals, such as Al and body-centred cube (bcc) iron, dislocation cross slip and local annihilations are

sufficiently easy to favour significant amounts of recovery. A classical example is the recovery of cold-drawn Al beverage cans during curing of the varnish at 150–200°C (Section 14.1). On the other hand, the low-SFE metals and alloys, e.g. rolled austenitic stainless steels and α-brass, do not undergo much recovery before recrystallization. This is also generally true for alloys with high solute contents, which reduce the dislocation mobility.

Though recovery is an important issue, it is often difficult to quantify. It can occur immediately after deformation, and also dynamically during deformation. Furthermore, recovery does *not* affect the optical microstructure or the crystallographic texture. Recovery affects properties such as hardness and structural features like, dislocation density, subgrain size and misorientation – but the resolution of such property changes is often poor and statistically quantifying the changes in the affected structural features is difficult.

5.2.1 Recovery mechanisms

The various mechanisms of recovery include (in order of increasing difficulty):

- point defect (vacancies and interstitials) annihilation by diffusion to sinks such as dislocations,
- mutual dislocation annihilation (closely spaced dislocations of opposite sign, or dipoles, which require small amounts of dislocation climb and/or cross slip),
- organization of free, random dislocations into dislocation walls or sub-boundaries (polygonization) (Cahn [1949], Kuhlmann-Wilsdorf [1989]) and
- coalescence of sub-boundary walls during subgrain growth.

The latter three mechanisms are illustrated schematically in Figure 5.2. Figure 5.3 illustrates an example of stored energy reduction in rolled high-purity iron by differential scanning calorimetry (DSC) (calorimetric) measurements at a constant heating rate. The diffuse recovery reaction extends over a wide temperature range before the sharper recrystallization peak.

Recovery mechanisms often operate simultaneously, so that there is no clear demarcation between them. For example, it is impossible to distinguish the collapse of diffuse dislocation cells into well-defined subgrain boundaries and subgrain growth.[2] This is one reason why recovery is difficult to treat analytically. Also, the mechanisms of the later stage of recovery, e.g. the formation of well-defined subgrains, are often the first stages of recrystallization nucleation which

---

[2] Owing to the heterogeneity of dislocation structures in deformed polycrystals, different recovery mechanisms may occur at different rates between different grains or between different parts of the same grain.
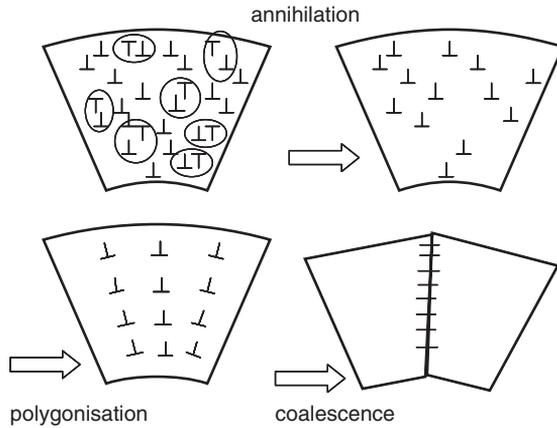
Figure 5.2. Schematic of successive dislocation annihilation mechanisms; cross-section of a bent crystal containing both free (edge) dislocations and dislocations, which accommodate the orientation gradient. During annealing, some dislocations anneal out by climb of opposite sign segments (encircled pairs) then the remainder rearrange into subgrain boundaries.
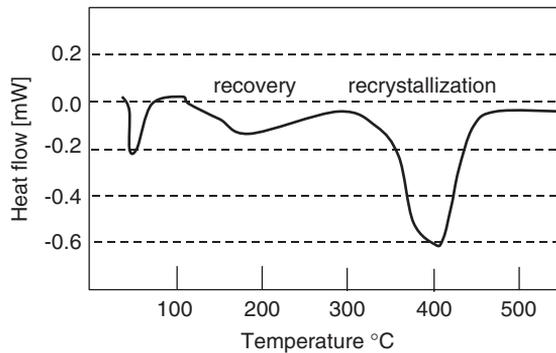
Figure 5.3. DSC plots at 20 K/min of ultrahigh purity Fe cold rolled 80% (Scholz *et al*. [1999]). Negative heat flows correspond to exothermic reactions, which are estimated at ≈ 4 J/mol for the recovery region (100–300°C) and 15 J/mol for recrystallization (320–450°C).

can lead to rapid recrystallization, stopping any further recovery. Finally, these fundamental mechanisms are also very sensitive to a wide variety of material parameters and processing conditions, such as deformation, temperature, etc.

As noted above, solute atoms play a major role in reducing defect mobility and therefore recovery kinetics. For example, deformed ultrahigh purity metals can recover at about $0.2T_m$ and start recrystallizing at $0.3T_m$ (see Figure 5.3). Solute atoms in commercial alloys push recovery and recrystallization temperatures to

0.4 and $0.6T_m$, respectively. This aspect has been analysed in detail by Nes [1995, 1997], and some parts of this analysis are described in Chapter 10 on modelling. Second phase particles, particularly as very fine distributions, will also inhibit recovery by pinning dislocations.

5.2.2 Recovery kinetics

Obtaining a generalized physical relationship for overall recovery kinetics is difficult. As the process involves several concurrent/consecutive mechanisms (Table 5.1), formulations of all the factors affecting recovery (Figure 5.2) and the heterogeneity of recovery are difficult and a comprehensive formulation does not exist.[3] Two empirical relationships are, however, often used to express the overall kinetics of recovery and denoted types 1 and 2 (Humphreys and Hatherly [1995]).

$$\text{Type 1: } \frac{dX}{dt} = \frac{-k_1}{t} \quad X = k_1' - k_1 \ln t \tag{5.1}$$

$$\text{Type 2: } \frac{dX}{dt} = -k_2 X^m \quad X^{(1-m)} - X_0^{(1-m)} = (m-1)k_2 t \tag{5.2}$$

where X is the fraction recovered (or change in recovery-dependent parameters – mechanical properties, resistivity or enthalpy), t is the annealing time and k_1, k_2 and m are the constants (k_1 and k_2 often scale with the activation energy of self-diffusion). Both relationships have been reported during recovery of single and polycrystalline metallic materials, but type 2 tends to be applicable for the special cases of single crystals with uniform substructures (and single mechanisms). Type 1 empirical kinetics are more typical of the complexities of deformed industrial alloys, where several recovery mechanisms can operate (Humphreys and Hatherly [1995]).

A more physically based kinetics analysis, first proposed by Kuhlmann *et al.* [1949] and later developed by Nes [1995], considers that the activation energy for the process increases during recovery as the internal stress, or the driving force, decreases. The easier, low energy, processes operate first and the higher activation energy mechanisms later, up to the value expected of atomic diffusion. If the activation energy for the process is written $U_F(X)$ and that for diffusion U_d then

$$\frac{dX}{dt} = -c \exp - \left\{ \frac{U_d - U_F(X)}{kT} \right\} \tag{5.3}$$

---

[3] The effect of recovery on microstructural developments is also difficult to translate into structure-dependent properties.

If $U_F(X)$ is a linear function, this gives a logarithmic time dependency for recovery of the form

$$X = 1 - \frac{kT}{A}\ln(1 + Bt) \tag{5.4}$$

where A and B are constants. This is similar to the type 1 kinetics of Eq. (5.1). The application of this type of analysis to the case of recovery controlled by solute atom diffusion is developed in more detail in Chapter 10.
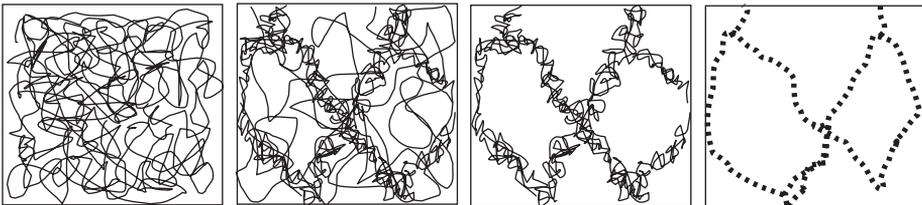
5.2.3 Structural changes during recovery

Apart from the initial and rapid loss of point defects, the main structural changes taking place during recovery can be categorized as:

- Rearrangement of dislocations into cellular structures (for high-SFE materials and most hot-deformed metals, this occurs simultaneously with deformation).
- Elimination of free dislocations within the cells.
- Collapse of the complicated dislocation cell walls into neat subgrain boundaries – mostly by annihilation of excess or redundant dislocations and rearrangement of the others into low-energy configurations (Figure 5.4).
- *Subgrain growth*. During continued annealing, an increase in subgrain size is theoretically expected since it leads to a reduction of internal energy. The experimentally observed kinetic relationships are usually written

$$d^n - d_0^n = k_3 t \tag{5.5}$$

where d and d_0 are the final and initial subgrain size, n, and k_3 are constants. While k_3 is strongly temperature-dependent (through the activation energy), values of n between 2 and 7 have been reported (Huang and Humphreys [2000]). There is a trend for the lower n values to be found in high-purity metals and at high temperatures, where sub-boundary mobility is the highest. Also, as

Figure 5.4. Schematics showing dislocation structure changes during recovery – random dislocation tangles through cell structures to subgrains.

discussed by Humphreys and Hatherly [1995], the *n* exponent may vary due to changes in the subgrain misorientation. Both average misorientation and the misorientation spread are reported to drop slightly and then remain stagnant during recovery, though there is also evidence of misorientation increase with recovery (Furu [1992]). A possible explanation is the role of orientation gradients, which tend to increase the average misorientation.

It should be pointed out that due to experimental difficulties in determing subgrain sizes with good accuracy – and therefore, their exact evolution during recovery before the onset of recrystallization – there have not been many detailed, quantitative studies of subgrain growth.

Another important aspect of recovery, with direct implication to recrystallization, is the issue of orientation dependence. This is also the least understood. Differences in stored energies, or in dislocation substructure, are often related to differences in Taylor factor (Kallend and Huang [1984], Samajdar and Doherty [1995], Rajmohan *et al*. [1997]) and also to differences in the so-called 'textural softening' (Cicalè *et al*. [2002]). Both are, however, related more to deformation than to recovery. The classical example is 'recovery' in rolled Cube {001}⟨100⟩ oriented grains of fcc metals. In this situation, the Burgers vectors of the active edge dislocations are perpendicular to each other, a particular case which avoids strong dislocation interactions and so facilitates rapid Cube recovery (Ridha and Hutchinsen [1982]) (see Figure 5.5).

The quantitative influence of recovery on softening is dependent on the relation between subgrain size and flow stress. The best fit for available experimental data on substructural strengthening (Thompson [1977], Gil Sevillano *et al*. [1980]) is obtained through a Hall–Petch type of relationship(s):

$$\sigma = \sigma_0 + k_5 d^{-c} \tag{5.6}$$

where σ is the yield stress, d the subgrain size, σ_0, k_5 and c are constants. The exponent c is equivalent to the classical Hall–Petch exponent; $c = -0.5$ for subgrains, which behave like grains, and $c = 1$ for low-energy dislocation substructure. The constant k_5 is also proportional to $(\theta)^{1/2}$, where θ is the average misorientation. It is, however, fair to point out that these generalized values or relationships are often not too consistent (Thompson [1977], Gil Sevillano *et al*. [1980]), making it difficult to relate recovery-induced structure with properties.

5.2.4 *Extended recovery/continuous recrystallization*

Standard recrystallization (Section 5.3) is a discontinuous process by which strain-free grains absorb deformed/recovered areas via high-angle grain boundary movement. As discussed in Section 5.1, this may severely limit recovery in the deformed
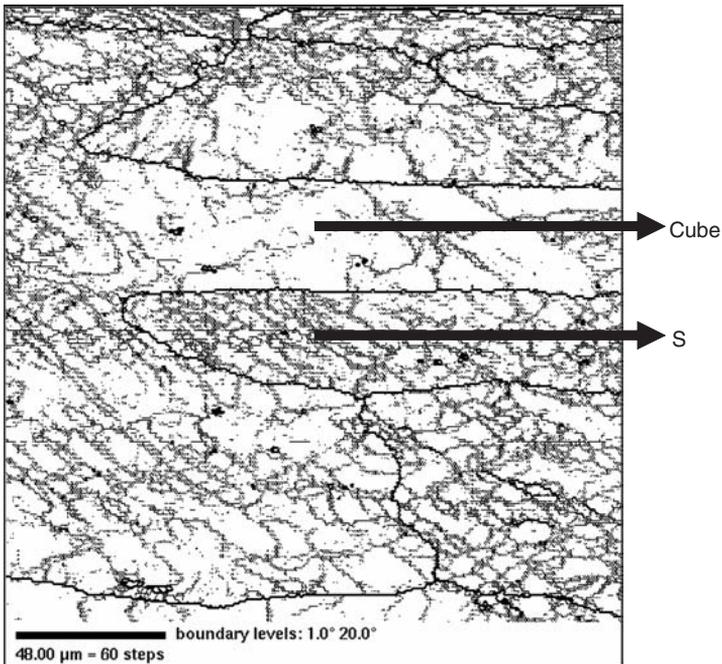
Figure 5.5. Difference in substructure between Cube {001}⟨100⟩ and S {231} ⟨346⟩ in aluminum – EBSD measurement on hot worked AA 1050 (Samajdar *et al*. [2001]).

areas. In certain circumstances, it is however possible to suppress discontinuous recrystallization, leading to a relatively fine and uniform grain size through 'homogeneous subgrain growth' – often termed 'extended recovery'. There is debate as to whether this is purely due to low-angle boundary movements or includes high-angle boundary migration. According to Humphreys and Hatherly [1995], the former is associated with extended recovey, while the latter leads to continuous recrystallization. These phenomena are observed locally (i.e. inside individual grains) as well globally (overall microstructural feature) and are discussed separately.

- *Local extended recovery*. This has been reported for aluminium (Hjelen *et al*. [1991]), low-carbon steel (Gawne and Higgins [1969], Samajdar *et al*. [1997b]) and Zr alloys (Vanitha [2006]) for grains of specific orientation families. These are often the grains/orientations free from strain localizations and hence subjected to homogeneous deformation.
- *Extended recovery/continuous recrystallization as an overall microstructural feature*. This has been reported in the following special circumstances.

- *Two-phase alloys*. Pinning by 2nd phase precipitates may stabilize subgrain structure and subsequent dissolution/coarsening of the precipitates may lead to 'homogeneous subgrain growth' or extended recovery (Humphreys and Hatherly [1995]), though the phenomena was originally identified in as *in situ* or continuous recrystallization (Köster and Hornbogen [1968]).
- Severe plastic deformation (Chapter 17.1) is often used to obtain ultrafine grain sizes through continuous recrystallization – static or dynamic. In such processes, severe plastic deformation and/or formation/dissolution of a 2nd phase are often used (Lee and McNelly [1987], Gudmundsson [1991], Humphreys and Bate [2001], Belyakov *et al*. [2002], Gholinia *et al*. [2002], Yu *et al*. [2004]). Such processes may involve extended recovery/continuous recrystallization as well as geometrical necessary dynamic recrystallization (Section 5.3.5.2). Recovery may also facilitate the formation of strain localizations, which, in turn, through developments of long-range misorientation may provide the appearance of grain-like structures under polarized light (which are indeed clusters of subgrains) (Samajdar *et al*. [1998d]).

5.3. RECRYSTALLIZATION

Primary recrystallization (also termed 'discontinuous recrystallization') is often 'viewed' as a nucleation and growth process. Though similar in name, and even partly in approach, to the nucleation and growth of phase transformation or solidification (see Section 2.2.1.1), there are significant differences. First of all, there is no 'classical' nucleation – the driving force of recrystallization being usually much smaller than that of 'classical' nucleation (Gottstein *et al*. [1985]). *The recrystallized nucleus is a part of the deformed matrix* (Humphreys and Hatherly [1995], Doherty *et al*. [1997]). In other words, any large subgrain or relatively well-recovered region of a deformed grain can be considered as a potential recrystallization nucleus – purely from the consideration of driving force, or relative differences in stored energy between the potential nucleus and its immediate surrounding. Whether such a potential nucleus is real or active will depend on its growth possibilities, particularly the presence of a growth-favourable[4] boundary. The velocity of such a boundary can be generalized as

$$V = MP \tag{5.7}$$

$$P = P_{SE} + P_C = (\alpha \rho G b^2) + \frac{2\gamma_b}{r} \tag{5.8}$$

---

[4] Recrystallization requires the presence and movement of high-angle boundaries. Their mobility is significantly larger than that of low-angle boundaries. Special boundaries (see Section 2.2.2.2), 27º $\langle 110 \rangle$ for bcc and 40º $\langle 111 \rangle$ for fcc, may have even higher mobility.

where *V*, *M* and *P* are respectively, the grain boundary velocity, mobility and the net pressure on the boundary. *P* has two components – P_{SE} or pressure due to the driving force or stored energy and P_C or pressure due to boundary curvature. The former can be given in terms of dislocation density[5] (α = constant close to 0.5, ρ = dislocation density, *G* = shear modulus and *b* = Burgers vector), while the latter can be obtained from the Gibbs–Thompson relation. γ_b and *r* are respectively the grain boundary energy and curvature, which is negative for expanding recrystallized grains (for more details on Gibbs–Thompson, the reader may refer Porter and Easterling [1986]).

A critically important aspect of this subject is the misorientaion dependence of boundary mobility (Humphreys [1995], Doherty [1997]). Low angle boundaries, such as those between sub-grains formed by deformation/recovery, have very low mobility, while boundaries with larger misorientations (>10–15º) have very high mobility. As a result, nucleation occurs by the rapid growth of a very small minority of sub-grains that evolve into growing new grains. The first necessary condition for this is that the sub-grain has, or quickly acquires, a local misorientation of more than 15º. The rapid growth of a very few sub-grains, compared to the slow growth of the remaining sub-grains, gives this common type of recrystallization its heterogeneous character – described as a "Nucleation and Growth" process.

Experimentally, it is impractical and impossible to exactly separate nucleation from growth. A region free from strain (e.g. without grain boundaries or misorientation) and exceeding a certain size (often based on the dimensions of the deformed grains) is considered as a recrystallized grain. To achieve this size, typically of the order of a micron, both nucleation as well as local or limited growth can be involved.

To identify the exact nuclei, or potential nuclei *just* turning active, is very difficult. In typical metallic systems, the size difference between the original subgrains (potential nuclei) and the final recrystallized grain is 10–100 times, making the probability of finding the exact nuclei in the deformed/recrystallizing matrix of the order of 10^{-3}–10^{-6}. Naturally, the focus of experimental research is often directed at identifying the recrystallization sources and also indexing and understanding their relative contributions to the recrystallized microstructure – size, shape and orientations of the recrystallized grains.

5.3.1 Sources of recrystallized grains

A summary of the typical, albeit generalized, recrystallization sources is given below.

---

[5] Strictly spoken, the difference in stored energy ($\rho - \rho_N$) should be considered, with ρ the dislocation density in the deformed zone and ρ_N the dislocation density in the growing nucleus, but in most cases one can consider ($\rho - \rho_N$) $\cong \rho$.
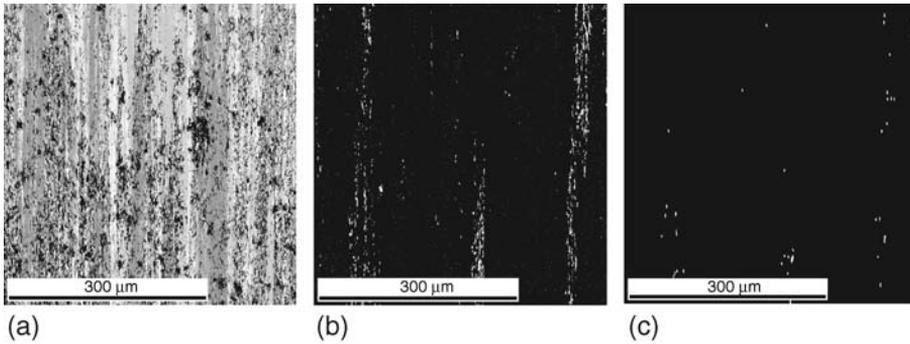
Figure 5.6. EBSD images of (a) hot deformed aluminium, (b) deformed Cube grain in (a), and (c) recrystallized Cube grain in (a). Distinction between (b) and (c) was established by considering grain orientation spread and grain size. A comparison of (b) and (c) indicates that the recrystallized Cube originate from deformed Cube. Courtesy Ravindra (IIT Bombay) – Research in Progress.

5.3.1.1 Deformed grains. As shown in Figure 5.6, a deformed grain may act as a source of recrystallized grains with more or less the same orientation as the 'mother' grain. Examples include Cube[6] recrystallization (Ridha and Hutchinsen [1982], Duggan *et al*. [1993], Samajdar *et al*. [1998d]) in fcc alloys and γ(ND//$\langle 111 \rangle$) fibre[7] recrystallization (Hutchinson [1984], Ray *et al*. [1994], Samajdar *et al*. [1999]) in low-carbon steel.

Cube recrystallized grains in fcc alloys originate from deformed Cube-oriented bands (see Figure 5.6). Such Cube bands, on the other hand, are suspected (Doherty *et al*. [1997], Samajdar *et al*. [1998e]) to be part of the original Cube-oriented grains in the undeformed structure. Cube grains nucleate favourable from the Cube bands, as the latter has lower stored energy (Ridha and Hutchinsen [1982], Doherty *et al*. [1997], Samajdar *et al*. [1998e]) and/or presence of growth favourable 40° $\langle 111 \rangle$ boundaries (Duggan *et al*. [1993]).

Recrystallized grains of γ(ND//$\langle 111 \rangle$) fibre in low-carbon steel also originate from deformed bands of similar orientation. Such bands are an effective recrystallization source due to extensive formation of grain interior strain localizations (Akbari *et al*. [1997]). The selective formation (Samajdar *et al*. [1999]) of strain localizations lead to fragmentation of the γ bands and correspondingly large variations in stored energy.

[6] Control of Cube recrystallization is the key issue in the TMP of both aluminium can stock (see Chapter 14.1), and of aluminium capacitor foils (see Chapter 14.2).

[7] Crucial for formablity of steel (see Chapter 11.10), and hence for the TMP of car body steel (see Chapter 15.1).

5.3.1.2 Shear bands. Shear bands cutting across several grains may also act as a source of recrystallized grains. The potency is often related to high stored energy and correspondingly large variations in relative misorientations and the possible presence of growth-favourable boundaries. Shear banding, briefly described in Section 4.2.1, is particularly strong in low-SFE metals and alloys. The formation of shear bands is often orientation sensitive (Dillamore *et al.* [1979], Gil Sevillano *et al.* [1980]); and hence, strong developments in recrystallization texture (preferred orientations of the recrystallized grains – for more details reader may refer Chapter 8) can be associated with recrystalliztion from shear bands.

5.3.1.3 Particle stimulated nucleation. Dislocations can be trapped by relatively large non-shearable particles (Ashby *et al.* [1970]). The dislocation density (ρ) around a particle is represented as

$$\rho = \frac{3F_{v}s}{rb} \tag{5.9}$$

where F_{v}, r, s and b are volume fraction and size of the of the 2nd phase particles, shear strain and dislocation Burgers vector. The entrapment and corresponding increase in dislocation density leads to the formation of a deformation zone – region around the 2nd phase particles with large misorientation developments. Though considerable efforts has been expended for modelling the deformed zones, a comprehensive physical model remains to be developed (Humphreys and Hatherly [1995]).

Recrystallization is favoured from particle-deformed zones due to large differences in the stored energies. Recrystallization of this type is referred as particle stimulated nucleation (PSN). The particle-deformed zones, and correspondingly the PSN grains, are of randomized orientations (Van Houtte [1995]).

In particle-containing commercial alloys, the annealing behaviour, including recrystallization texture developments, is strongly influenced by annealing temperature. Low-temperature annealing is often related to stronger randomization (Ørsund and Nes [1988], Samajdar *et al.* [1998c]). To explain such behaviour, two approaches have been proposed. The first approach (Ørsund and Nes [1988]) assumes the presence of inner and outer deformed zones – the former being more randomized. The annealing temperature is expected to determine the relative contributions from the zones and in turn decides the recrystallization behaviour. An alternative approach (Samajdar *et al.* [1998c]) proposes that the relative contributions from PSN and deformation bands are responsible

for the overall recrystallization behaviour, including recrystallization texture developments.

5.3.1.4 Recrystallization twins. This is more valid for lower-SFE metals and alloys – e.g. copper, austenitic stainless steel (see Chapter 17.2), etc. Multiple twinning in the early recrystallization stages has been reported (Berger *et al*. [1988]) to play an important role in determing the orientations of the recrystallized grains. In the real sense this is not a true recrystallization source, but the only mechanism which may form recrystallized grains with new orientations – orientations otherwise absent in the deformed matrix.

5.3.2 Recrystallization mechanisms

Developments in recrystallized microstructures depend on the nucleation and growth of the recrystallized grains. While nucleation can be generalized as relative activation of different recrystallization sources, strain-free nuclei consume the deformed matrix during the growth process. The patterns of recrystallization, including recrystallized microstructure, are decided by the relative advantange/ disadvantage of nucleation and growth.

The advantage/disadvantage relations of nucleation and growth are often generalized as ON (oriented nucleation) and OG (oriented growth) respectively, representing preferred nucleation and growth (Doherty [1985], Humphreys and Hatherly [1995], Doherty *et al*. [1997]). This distinction has one major problem – it is difficult to make a precise demarcation between the nucleation and growth stages of recrystallization. An alternative is to describe the developments in recrystallized microstructure, especially recrystallization texture, in terms of frequency and size advantage of recrystallized grains of different orientations (Doherty [1985]). Thus, if the volume fraction of a particular component *i* increases during recrystallization, then such an increase has to be due to larger number of *i* recrystallized grains and/or their bigger sizes. Frequency (α) and size (β^3) advantage factors are described as

$$\alpha = \frac{i_{rex}}{i_{random}} \tag{5.10}$$

$$\beta^3 = \left(\frac{D_i}{D_{average}} \right)^3 \tag{5.11}$$

where i_{rex} and i_{random} are the respective number fraction of *i* grains in the recrystallized material and in a random texture; D_i and $D_{average}$ are the mean grain sizes

Table 5.3. Summary of the micromechanisms responsible for frequency/size advantage.

Frequency advantage	*Stored energy advantage*: Nucleation of a particular recrystallization source and/or orientation may be preferred. The preference is typically caused by large variation of stored energy within the source (example: recrystallization from deformed γ fibre bands in bcc steel (Hutchinson [1984], Ray *et al*. [1994], Samajdar *et al*. [1999])) or between the source and the surrounding (example: recrystallization from Cube bands in fcc alloys (Ridha and Hutchinsen [1982], Duggan *et al*. [1993], Samajdar *et al*. [1998d]))
	Micro growth selection: Presence of growth-favourable boundaries to intiate preferred nucleation (example: presence of 40º ⟨111⟩ boundary or S next to deformed Cube in fcc alloys (Duggan *et al*. [1993]))
Size advantage	*Growth advantage/disadvantage*: Unlike single crystals, in heavily deformed polycrystalline material, a global growth advantage is controversial (Doherty *et al*. [1997]) – as the nature of the grain boundary between a recrystallized grain and the deformed matrix is expected to change many times. Growth disadvantage (Section 5.3.4) through particle pinning and/or orientation pinning may, however, lead to a size disadvantage
	Early nucleation: Early preferential nucleation can also lead to size advan tage (example: large Cube grain in fcc aluminium was reported to be caused by early nucleation (Samajdar *et al*. [1998e]) – the estimated growth velocity of Cube and non-Cube being similar)

for i and average (i.e. irrespective of any crystallographic orientation) grains. Assuming spherical grain shape, the size advantage factor was taken as β^3 (Doherty [1985]). Evidently, the recrystallization texture will be strengthened when α and/or β^3 are larger than 1.

Such an approach relates directly to recrystallized microstructures and stays clear from the ON and OG models, a subject of nearly half century old debates and discussions (for more details on ON and OG, the reader may refer to Section 8.4.2). Table 5.3 summarizes the micromechanisms responsible for the frequency and size advantages. As shown in the table, the frequency advantage can be caused by both preferred nucleation and/or micro growth advantage – the latter can be considered as part of the early nucleation process. The size advantage, on the other hand, has been attributed to growth advantage/disadvantage and/or early nucleation.

Any discussion of recrystallization micromechanisms remains incomplete without describing further the mechanisms behind stored energy and growth advantage/disadvantage. The stored energy advantage/disadvantage, or differences in stored energy in different grains or orientations, is caused by deformation and orientation-dependent recovery – a topic described earlier in Section 5.2.3. The

growth advantage/disadvantage, on the other hand, depends on the effects of 'pinning' on different types of grain boundary. While differences in grain boundary nature have been covered in Section 2.2.2.2, the present section tries to summarize three different types of grain boundary 'pinning'.

- *Particle Pinning or Zener Drag*. The pinning pressure (P) is given as

$$P = \frac{3F_v\gamma}{2r} \tag{5.12}$$

  where F_v, r and γ are particle volume fraction, particle size and grain boundary energy, respectively. Low-energy boundaries, such as low coincidence site lattice (CSL) boundaries, have low-Zener drag.
- *Solute drag*. The presence of solute is also expected to have a retarding effect on growth – the so-called solute drag (Lücke and Stüwe [1963], Gordon and Vandermeer [1966], Dimitrov *et al*. [1978]). The solute drag is lower for low-CSL boundaries.
- *Orientation pinning*. A growing recrystallized grain can be pinned by a deformed region of similar orientation (Juul Jensen [1995]) – i.e. by the presence/occurance of a low-angle boundary. Orientation pinning has been reported to have strong influence in both fcc Cube recrystallization (Doherty *et al*. [1997]) and in γ fibre recrystallization of low-carbon steel (Samajdar *et al*. [1999]).

5.3.3 Recrystallization kinetics

The analysis of recrystallization kinetics is often based on one of two tools – JMAK (Johnson, Mehl, Avrami, Komogorov) analysis and the microstructural path methodology (MPA). JMAK[8] relates the fraction recrystallized with time (t) as

$$1 - \exp\left(-kt^n\right)$$

where k is a constant and n the JMAK exponent. The JMAK exponent can be used to get a feel for the overall recrystallization kinetics. For example in a three-dimensional (3D) structure, theoretical n values of 3 and 4, respectively correspond to site saturation (nucleation happening at one instant) and to a constant nucleation rate (Humphreys and Hatherly [1995]). n can also be used to index sluggish growth or delayed nucleation. Random nucleation is critical for the validity of JMAK analysis. For example, fine-grained copper with random nucleation follows ideal JMAK, but the coarse-grained material does not (Hutchinson [1989]).

---

[8] Chapter 10 (Section 10.2.1) describes the JMAK analysis in details.

In fine-grained material, less than one successful nucleation from each deformed grain is expected, effectively randomizing the spatial distribution of the nuclei.

MPA attempts to extract the nucleation and growth rates from the experimental data. The primary problem of estimating nucleation rates from two-dimensional (2D) microstructural observations is circumvented by using the Laplace transform (Gokhale and Dehoff [1989], Vandermeer and Rath [1989]), and nucleation and growth rates are estimated as direct output.[9] For isothermal annealing without any shape change for the recrystallizing grains, the nucleation rate (N_τ, nucleation rate at a time instant τ) and the grain size (D – major axis of spheroidal grains) can be expressed as

$$N_\tau = N_1 t^{\delta\text{-}1} \tag{5.13}$$

$$D_{(t-\tau)} = G(t - \tau)^r \tag{5.14}$$

where N_1, δ, G and r are constants, t is the time and G is the growth rate. Though MPA is capable of separating out the nucleation and growth from experimental data, both JMAK and MPA are usually restricted by the basic assumption of random nucleation.

5.3.4 Role of second phase
Table 5.4 outlines the possible effects of different types of 2nd phase particles on the recrystallization behaviour. As shown in the table, the effects of 2nd phase particles can be generalized as (i) nucleation advantage[10] through PSN and/or nucleation on particle-induced strain localizations and (ii) growth disadvantage through particle pinning or Zener drag. The latter can be used effectively to control the grain size in a particle-containing alloy. The 'pinning' limited grain size (D_{Zener}) is often approximated as

$$D_{\text{Zener}} = \frac{4r}{3F_v} \tag{5.15}$$

where r and F_v are the particle size and volume fraction, respectively.

---

[9] It is to be noted that the original methodology was proposed by Gokhale [1985] for estimating nucleation rates during classical phase transformation. This was adopted for recrystallization by Vandermeer [1989].

[10] Nucleation disadvantage may come indirectly through inhibition of recovery during simultaneous precipitation.

Table 5.4. Effects of different types of 2nd phase particles on recrystallization.

| Nature of the particle	Nucleation	Growth
Non-shearable particles	*Nucleation advantage*: For large particles – PSN; also possible is nucleation on particle-induced strain localizations	Particle pinning or Zener drag – growth disadvantage
Fractured particles	Small plate-shaped carbides may undergo (Kamma and Hornbogen [1976]) fracture and initiation of strain localizations. The latter may aid nucleation	Particle pinning or Zener drag – growth disadvantage
Coherent particles	No effect – small particles	Zener drag and growth inhibition – example: coherent precipitates in Cu−3%Co alloys (Phillips [1966])
Semi-shearable particles	No effect – soft 2nd phase does not form deformed zones or strain localizations	Zener drag and growth inhibition, especially dominant in regions with 2nd phase continuity
Shearable particles	No effect	Zener drag – example: pores and gas bubbles
Simultaneous precipitation	Depending on annealing conditions and precipitation kinetics, recovery and hence nucleation can be hindered	Depending on annealing conditions and precipitation kinetics, Zener drag and growth inhibition

5.3.5 Dynamic recrystallization

Under certain conditions, the structure can recrystallize during deformation giving rise to dynamic recrystallization. In principle, this form of recrystallization can also occur during cold deformation, but in practice, this is only exceptionally observed, e.g. in very pure metals. In this section, dynamic recrystallization is classified as either discontinuous dynamic recrystallization (Derby [1987, 1991]) or as one of two other types. The latter are geometric dynamic recrystallization (McQueen *et al*. [1989]) and dynamic recrystallization through progressive sub-grain rotation (Gardner and Grimes [1979]), and both involve strain-induced phenomenon with limited or no movements of high-angle boundaries. Following usual practice, these other types have been included here as part of the present section on dynamic recrystallization.

5.3.5.1 Discontinuous dynamic recrystallization.

Figure 5.7 shows typical flow curves during cold and hot deformation. During hot deformation, the shape of the flow curve can be 'restricted', or work hardening rates counterbalanced, by
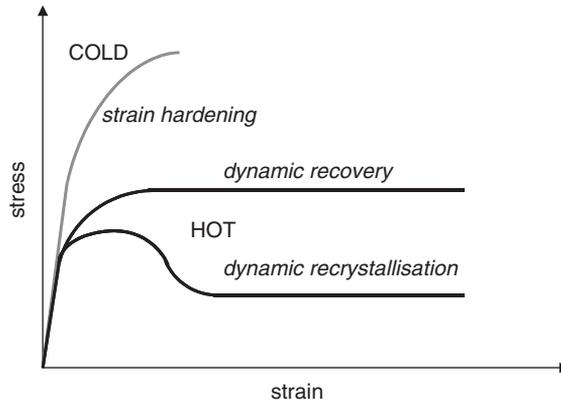
Figure 5.7. Typical flow curves during cold and hot deformation.
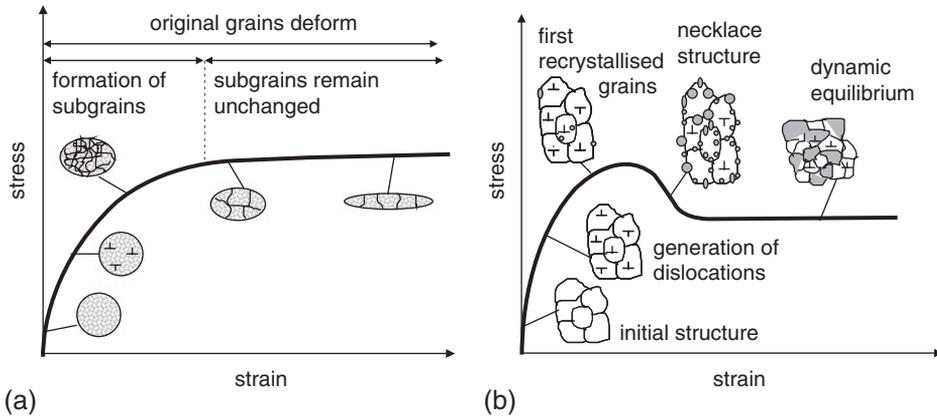
Figure 5.8. Evolution of the microstructure during (a) hot deformation of a material showing recovery and (b) dynamic recrystallization or discontinuous dynamic recrystallization.

dynamic recovery or by dynamic recrystallization (i.e. discontinuous dynamic recrystallization). Dynamic recovery is typical of high-SFE metals (e.g. aluminium, low-carbon ferritic steel, etc.), where the flow stress saturates after an initial period of work hardening. This saturation value depends on temperature, strain rate and composition. On the other hand, as shown in Figure 5.7, a broad peak (or multiple peaks) typically accompany dynamic recrystallization.

Figure 5.8 illustrates schematically the microstructure developments during dynamic recovery and dynamic recrystallization. During dynamic recovery, the original grains get increasingly strained, but the sub-boundaries remain more or

less equiaxed. This implies that the substructure is 'dynamic' and re-adapts continuously to the increasing strain. In low-SFE metals (e.g. austenitic stainless steel, copper, etc.), the process of recovery is slower and this, in turn, may allow sufficient stored energy build-up. At a critical strain, and correspondingly at a value/variation in driving force, dynamically recrystallized grains appear at the original grain boundaries – resulting in the so-called 'necklace structure'. With further deformation, more and more potential nuclei are activated and new recrystallized grains appear. At the same time, the grains, which had already recrystallized in a previous stage, are deformed again. After a certain amount of strain, saturation/equilibrium sets in[11](see Figure 5.8b). Typically equilibrium is reached between the hardening due to dislocation accumulation and the softening due to dynamic recrystallization. At this stage, the flow curve reaches a plateau and the microstructure consist of a dynamic mixture of grains with various dislocation densities.

It is important, at this stage, to bring out further the structural developments and structure–property correlation accompanying dynamic recovery and dynamic recrystallization respectively. Both the subgrain size ($d_{subgrain}$, from dynamic recovery) and grain size (D_{rex}, dynamic recrystallization) are increasing functions of temperature and of inverse strain rate. Both follow a Hall–Petch-type (Eq. (4.3)) relationship.

$$\sigma = \sigma_1 + k_1 (d_{subgrain})^{n_1} \tag{5.16}$$

$$\sigma = \sigma_2 + k_2 (D_{rex})^{n_2} \tag{5.17}$$

where σ is flow stress and σ_1, k_1, n_1, σ_2, k_2 and n_2 are constants. Corresponding to dynamic recovery (Eq. (5.16)), σ_1 has a low value and n_1 is close to 1, while k_1 depends on alloy composition (being higher at higher solute content). For dynamic recrystallization (Eq. (5.17)), n_2 typically falls within 0.5–0.8.

Unlike static and dynamic recovery, recrystallization includes another classification – a sort of grey area between dynamic and static: meta-dynamic recrystallization. In this situation, the recrystallized nuclei form or nucleate dynamically, during hot deformation, but growth takes place during subsequent static annealing.

5.3.5.2 *Other types.*
- *Geometric dynamic recrystallization*. Grains with serrated boundaries (see Figure 5.9), a by-product of dynamic recovery, may pinch each other when subgrain size approaches the grain thickness. Such a mechanism (McQueen *et al*. [1989]) can

---

[11] Because of the dynamic recrystallization, the material becomes softer, with corresponding appearance of a broad peak in the flow stress (see Figure 5.7).

380 μm
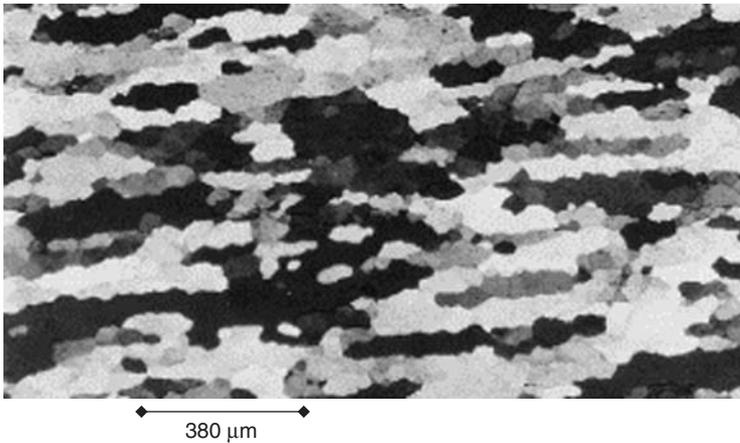
Figure 5.9. Polarized light optical image of hot deformed aluminium showing serrated grain boundaries (Samajdar *et al.* [2001]).

produce microstructures appearing 'recrystallized' (e.g. dynamically recrystallized), but this structure is more a product of deformation and recovery.

- *Dynamic recrystallization through progressive subgrain rotation*. This was originally reported for geological formations as rotational recrystallization, and was subsequent observed in high solute metals (Gardner and Grimes [1979]). During deformation, subgrains in the neighbourhood of pre-existing boundaries may undergo significant higher rotations than the grain-interior subgrains. At large strain, high-angle boundaries may develop. Though the exact mechanism is not fully understood, it is normally believed (Humphreys and Hatherly [1995]) to involve a combination of inhomogeneous plastic deformation, accelerated dynamic recovery in near-grain boundary regions and grain boundary sliding.

5.4. GRAIN COARSENING

Post recrystallization grain growth is driven by the surface energy or the grain boundary energy and this driving force is about two orders of magnitude lower than that of recrystallization. Though often called grain growth, the term grain coarsening is preferable – parity with interfacial energy driven precipitate coarsening[12].

Grain coarsening can occur in two forms: normal and abnormal[13]. In normal grain coarsening, the central mechanism is the loss of the smallest grains, while

---

[12] As in Chapter 7, interfacial energy driven precipitate coarsening (or competitive growth) is distinguished from supersaturation driven precipitate growth.
[13] also called secondary recrystallization

maintaining a nearly constant grain size distribution. In abnormal grain coarsening a few grains grow into a pinned grain structure. The pinning occurs usually by particles or by a high frequency of low angle, and thus low mobility, boundaries. In the present section on grain coarsening, some of the theories/models are highlighted first, followed by a brief summary of the factors affecting grain coarsening.

5.4.1 Theories of Grain Coarsening
Table 5.5 makes an attempt to collate some of the important theories of grain coarsening. As shown in the table, the theories and models range from fairly simple early statistical theories (Burke [1952]) to more complex statistical (Hillert [1965], Rhines [1974], Abbruzzese [1986], Mullins [1989a, 1989b]) and deterministic (Atkinson [1988], Anderson [1989]) models available today. The list (Table 5.5) is not an exhaustive one. For more details, the reader may refer to Atkinson [1988], Humphreys [1995] and Martin [1997].

It is important to point out that the statistical theories need to take simplifying assumptions, while the deterministic models are often too computation intensive. Even in primarily single phase metals, the model predictions and the experimental results often may not tally[14] – such differences are attributed to different factors: solute drag, Zener pinning, differences in grain–grain boundary mobilities and initial grain structure being different form the ideal one (i.e. non-equiaxed grains and/or different grain size distribution).

5.4.2 Factors affecting grain growth
The factors affecting grain growth are given below.

- *Specimen size*. The driving force is significantly reduced when grain size approaches ½ thickness of the specimen. The effect is due to reduced curvature of the grain boundary, since at the equilibrium grain boundaries must fall normally onto the sample surface. In addition, at grain boundary intersection with the surface, grooves form, further hindering boundary migration.
- *Temperature*. Grain boundary mobility depends strongly on the temperature (a Arrhenius-type relationship) and in turn affects grain growth kinetics. Another indirect effect of temperature is through dissolution/coarsening of 2nd phase particles pinning grain boundaries.

---

[14] And it is impossible to pin-point the best theory or model. The basic model assumptions, for some of the earlier model (see Martin [1997]) can also be debated. Mullins W.W., Acta Metall., 37 (1986b), 2979.

Table 5.5. Summary of some of the important theories/models of grain growth.

General classification	Model details	Remarks
Statistical models	*Burke [1952]:* Driving force $= P = \{(2\gamma)/R\}$ where γ and R are the grain boundary energy and radius of curvature	Offers only average grain size and not a distribution
	Average grain size at time $t = R_{av} = ct^{1/n}$. c is a constant and n is the grain growth exponent	Simplistic, yet relevant
	Deviation from an ideal exponent of 2 is observed even in pure metals – often explained from variations in boundary mobility (due to solute drag) and the presence of 'limiting' grain size (Zener pinning)	
	Feltham [1957] and Hillert [1965]: $dR_c/dt = (c_1 M\gamma)/(4R_c)$. R_c is a critical radius below and above of which grains would respectively, shrink or grow. c_1 is a shape factor (0.1 and 1 for 2D and 3D) and M is the boundary mobility	Parabolic growth kinetics
	Rhines [1974]: Considers the role of topology. Modified Rhines analysis: $V_{av} = V_0 + ct$; where V_0 and V_{av} are the mean grain volume at time instance 0 and t	Growth exponent of 3 is predicted
	Abbruzzese [1986]: 2D topological model using an experimental relationship between grain sides/facets and grain size	Parabolic growth kinetics
	Mullins [1989a, 1989b]: Parabolic coarsening kinetic was established, provided (i) rate controlling boundary mobility and (ii) grain size distribution normalized by the time dependent average grain size remain constant	Perhaps the most important analysis on the statistical approach.
Deterministic models	*Equation of motion – Atkinson [1988]:* Intial grain structure is allowed to stabilize/equilibrate (based on some governing equations) by several iterations	Parabolic kinetics; sensitive to starting structure
	Monte Carlo – Anderson [1989]: Use of Monte Carlo algorithm in grain growth simulation is a relatively mature subject	Growth exponent approaching 2

- *Initial structure.* The initial structure, especially the shape (topological effects) and the grain size distribution (Eqs. (5.18) and (5.19)) can have very strong influence on the grain growth. The grain size distribution (represented by a distribution function $f(D)$) is often generalized as log-normal or Rayleigh type, the former being more relevant to experimental data. Changes

in the distribution at the initial stages or during grain growth can affect the growth significantly:

$$\text{Log normal distribution: } f(D) = k_1 \exp(-(\ln D)^2) \qquad (5.18)$$

$$\text{Rayleigh distribution: } f(D) = k_2 \exp(-k_3 D^2) \qquad (5.19)$$

where k_1, k_2 and k_3 are constants.

- *Pinning*. Primarily the pinning is caused by solute drag, Zener pinning and orientation pinning (see Section 5.3.2). Whatever the source, the extent of pinning often differs between different types of grain boundaries. Whatever might be source, extent of pinning often gives rise to different mobilities of different types of grain boundaries. As a result, the relative presence of growth-favourable (low-CSL boundaries) and non-favourable (low-angle boundaries) boundaries may have significant effects on grain coarsening. The problem, however, is a complex one – as the relative presence of different types of boundaries may change significantly during grain growth.

As a result of these complications, the actual kinetic of grain coarsening cannot yet be reliably predicted in any given microstructure. Nor is it known how, why or after what time of annealing abnormal coarsening can occur in a pinned grain structure.

LITERATURE

Doherty R.D., Prog. Mater. Sci., 42 (1997), 39.
Doherty R.D., Hughes D.A., Humphreys F.J., Jonas J.J., Juul Jensen D., Kassner M.E., King W.E., McNelley T.R., McQueen H.J. and Rollet A.D., Mater. Sci. Eng., A238 (1997), 219.
Humphreys F.J. and Hatherly M., "Recrystallization and Related Annealing Phenomena", Elsevier, UK (1995).